Geophys. Astrophys. Fluid Dynamics, Vol. 51, pp. 103–133
Reprints available directly from the publisher
Photocopying permitted by license only

ON OPEN BOUNDARY CONDITIONS FOR THREE DIMENSIONAL PRIMITIVE EQUATION OCEAN CIRCULATION MODELS

DAVID P. STEVENS

School of Mathematics, University of East Anglia, Norwich NR4 7TJ, U.K.

(*Received 8 February 1989; in final form 11 May 1989*)

An open boundary condition is constructed for three dimensional primitive equation ocean circulation models. The boundary condition utilises dominant balances in the governing equations to assist calculations of variables at the boundary. The boundary condition can be used in two forms. Firstly as a passive one in which there is no forcing at the boundary and phenomena generated within the domain of interest can propagate outwards without distorting the interior. Secondly as an active condition where a model is forced by the boundary condition. Three simple idealised tests are performed to verify the open boundary condition, (1) a passive condition to test the outflow of free Kelvin waves, (2) an active condition during the spin up phase of an ocean, (3) finally an example of the use of the condition in a tropical ocean.

KEY WORDS: Ocean circulation, open boundaries, primitive equations.

1. INTRODUCTION

In an ideal world, modellers would have unlimited computer power to aid modelling and understanding of the world's entire oceans. At present this is not the case and thus we have to turn our attention to limited areas to stay within the bounds set by available computing power. If the model were perfect and we had an exact knowledge of all the fields at the open boundaries along with their variation with time, then all we would need to do is to prescribe these values. This would lead to a perfectly well posed mathematical problem. Unfortunately models are not perfect, as for example discretisation always introduces errors. It is also likely that we will never be able to get good enough data for boundary conditions. Heat, salt and momentum are advected inwards for regions on the boundary where the flow is into the model domain. In this situation it is possible to specify mean observed values for these fields as they should give a reasonable estimate. However difficulties occur in regions where the flow or wave propagation is out of the domain of interest. A prescribed value, if fixed, can cause problems as the fluid advected toward the boundary could have a totally different temperature or salinity to that on the boundary, leading to large variations in either quantity in that region, which in turn could lead to unrealistic pressure gradients. Also there is a need to make sure any signal travelling towards these open boundaries is

transmitted and not reflected back into the region of interest. Thus at open boundaries an unphysical condition is required, usually based on some form of extrapolation.

Coverage of the open boundary problem in the literature is limited to meterological problems, shelf sea models and reduced physics ocean problems such as shallow water equation, single layer reduced gravity (Camerlengo and O'Brien, 1980) and quasi-geostrophic (Verron, 1986) models. Open boundaries for three dimensional primitive equation models have received little attention. Many open boundary conditions used are based on the Sommerfeld radiation condition, for example Orlanski (1976). However this condition is not valid if the model is forced close to the boundary. Also problems can occur with Rossby waves at open boundaries using radiation conditions, as in general the phase and group velocity of such waves are not parallel. Røed and Smedstad (1984) split their linear shallow water equations into two sets; one which is satisfied by a local forced mode and one which is satisfied by a global mode that can be described by free wave equations. However they require the forcing near the boundary to be independent of the coordinate normal to that boundary. Others have used so-called sponge layers for their limited area studies, for instance the quasi-geostrophic models of Holland (1986), Røed and Cooper (1986) review a number of open boundary conditions that have been used to date. The open boundary problem was shown to be ill-posed by Bennett and Kloeden (1978), who considered the barotropic filtered equations in detail. The problem occurs at points on the boundary where the flow is tangential. Even though the problem is ill-posed some ground can still be gained by using open boundaries.

There are two types of open boundary condition that the oceanographic modeller is likely to come across. Passive open boundary conditions where there is no forcing at the boundary. Here all the boundary condition is required to do is to let phenomena generated within the domain of interest propagate out without reflecting or distorting. The other kind of open boundary condition is an active one in which case the boundary condition actively forces the interior solution. However, disturbances must still be able to leave the region of interest without distorting the interior or creating problems near the boundary. The open boundary condition was originally constructed for use with a three dimensional primitive equation model of the Norwegian and Greenland seas. However the boundary condition should be widely applicable, as is demonstrated in Sections 5, 6 and 7. Numerical analysis of the complex nonlinear problem at open boundaries is an intractable problem. Thus a pragmatic approach will be adopted, illustrating the use of the condition in idealised test cases.

2. THE MODEL AND NATURAL BOUNDARY CONDITIONS

The open boundary condition was constructed for use in an ocean general circulation model based on that of Cox (1984) in which the equations of motion, temperature and salinity are solved on a finite difference grid. In this model the full equations are

$$\frac{\partial u}{\partial t}+\Gamma(u)-fv=-\frac{1}{\rho_0 a\cos\phi}\frac{\partial p}{\partial\lambda}+F^u, \tag{1}$$

$$\frac{\partial v}{\partial t}+\Gamma(v)+fu=-\frac{1}{\rho_0 a}\frac{\partial p}{\partial\phi}+F^v, \tag{2}$$

$$\frac{\partial p}{\partial z}=-\rho g, \tag{3}$$

$$\Gamma(1)=0, \tag{4}$$

$$\frac{\partial T}{\partial t}+\Gamma(T)=F^T, \tag{5}$$

$$\rho=\rho(\theta,S,z), \tag{6}$$

where

$$\Gamma(\mu)=\frac{1}{a\cos\phi}\frac{\partial}{\partial\lambda}(u\mu)+\frac{1}{a\cos\phi}\frac{\partial}{\partial\phi}(v\mu\cos\phi)+\frac{\partial}{\partial z}(w\mu),$$

$$F^u=K_m\frac{\partial^2 u}{\partial z^2}+A_m\left(\nabla^2 u+\frac{(1-\tan^2\phi)u}{a^2}-\frac{2\sin\phi}{a^2\cos^2\phi}\frac{\partial v}{\partial\lambda}\right),$$

$$F^v=K_m\frac{\partial^2 v}{\partial z^2}+A_m\left(\nabla^2 v+\frac{(1-\tan^2\phi)v}{a^2}+\frac{2\sin\phi}{a^2\cos^2\phi}\frac{\partial u}{\partial\lambda}\right),$$

$$F^T=K_h\frac{\partial^2 T}{\partial z^2}+A_h\nabla^2 T,$$

and

$$\nabla^2(\mu)=\frac{1}{a^2\cos^2\phi}\frac{\partial^2\mu}{\partial\lambda^2}+\frac{1}{a^2\cos\phi}\frac{\partial}{\partial\phi}\left(\frac{\partial\mu}{\partial\phi}\cos\phi\right).$$

The variables $\phi,\lambda,z,u,v,w,p,\rho$ represent latitude, longitude, depth, zonal velocity, meridional velocity, vertical velocity, pressure and density respectively. The radius of the Earth is a, g is the acceleration due to gravity, ρ_0 is a reference density and $f=2\Omega\sin\phi$ is the Coriolis parameter where Ω is the speed of angular rotation of the Earth. The variable T represents any tracer including active tracers such as potential temperature θ and salinity S or passive tracers such as tritium. A_m and

A_h are the horizontal mixing coefficients for momentum and tracers. K_m and K_h are the corresponding vertical mixing coefficients.

The equations of motion are rearranged to form an equation for the barotropic stream function ψ

$$\left[\frac{\partial}{\partial\lambda}\left(\frac{1}{H\cos\phi}\frac{\partial^2\psi}{\partial\lambda\partial t}\right)+\frac{\partial}{\partial\phi}\left(\frac{\cos\phi}{H}\frac{\partial^2\psi}{\partial\phi\,\partial t}\right)\right]-\frac{\partial}{\partial\lambda}\left(\frac{f}{H}\frac{\partial\psi}{\partial\phi}\right)-\frac{\partial}{\partial\phi}\left(\frac{f}{H}\frac{\partial\psi}{\partial\lambda}\right)\Bigg]$$

$$=-\left[\frac{\partial}{\partial\lambda}\left(\frac{g}{\rho_0 H}\int_{-H}^{0}\int_{z}^{0}\frac{\partial\rho}{\partial\phi}dz'\,dz\right)\right.$$

$$\left.-\frac{\partial}{\partial\phi}\left(\frac{g}{\rho_0 H}\int_{-H}^{0}\int_{z}^{0}\frac{\partial\rho}{\partial\lambda}dz'\,dz\right)\right]$$

$$+\left[\frac{\partial}{\partial\lambda}\left(\frac{a}{H}\int_{-H}^{0}F^v-\Gamma(v)\,dz\right)\right.$$

$$\left.-\frac{\partial}{\partial\phi}\left(\frac{a\cos\phi}{H}\int_{-H}^{0}F^u-\Gamma(u)\,dz\right)\right], \tag{7}$$

where

$$-\frac{1}{a}\frac{\partial\psi}{\partial\phi}=\int_{-H}^{0}u\,dz,\quad\frac{1}{a\cos\phi}\frac{\partial\psi}{\partial\lambda}=\int_{-H}^{0}v\,dz.$$

Details of the equations for the baroclinic velocities and the method of solution have been given by various authors [Bryan (1969), Semtner (1974), Cox (1984) and Semtner (1986)]. The finite difference grid used is that of the Arakawa "B" type, in which tracer points T and stream function points ψ are placed in the centre of cells and the horizontal velocity components u, v are situated at the corners. In the vertical T, u, v are located in the centre of the cell. Time stepping is achieved by leapfrogging, with the associated time splitting removed by a Robert time filter as described by Asselin (1972).

At the surface the model is driven by a prescribed wind stress and buoyancy flux. The usual no slip and no flux of tracer conditions are applied at side walls, along with free slip and a no flux of tracer condition at the ocean floor. Further details of the boundary conditions used have been given in the above four articles.

3. OPEN BOUNDARY CONDITIONS

The values of variables at open boundary points would be described by the equations of motion if the model boundary were extended. Thus it would seem sensible to use these equations or at least their dominant terms to describe

variables at open boundaries. The reason why the Sommerfeld radiation condition works well in some problems is because it captures the dominant physics, that is the propagation of a quantity out of the domain of interest. However this condition is not always the best balance of terms in the equations for all problems, as will be seen below. The method suggested here is as follows. For simplicity a southern open boundary will be described. However the scheme could be used for any orientation of the boundary.

Providing a condition for the barotropic stream function gives the most difficulty. There are very few useful simplifications of the elliptic equation (7) describing the stream function, that are tractable along an open boundary. In an active open boundary condition where there is wind forcing right up to the boundary, the stream function can be calculated from the Sverdrup balance

$$\frac{\partial \psi}{\partial \lambda} = -\frac{a}{2\Omega \cos\phi}\left(\frac{\partial}{\partial \phi}(\tau^{\lambda}\cos\phi) - \frac{\partial \tau^{\phi}}{\partial \lambda}\right), \tag{8}$$

provided a western boundary current is imposed to ensure conservation of mass. Although this is a steady equation, the external mode responds quickly to any change in wind forcing, and thus this balance should provide a reasonable estimate. Any inflows or outflows, produced by effects outside the region of interest, that are required must be prescribed from observations or possibly data from a coarse grid model covering a larger domain. There is no useful way of simplifying the elliptic barotropic stream function equation for use with a passive open boundary. In this situation information is propagating outwards from the model interior; no information comes from the boundary. The best way forward is to allow the stream function to be freely modified by some form of extrapolation, such as that described in Section 4. Although this is mathematically ill posed, in practice reasonable results are obtained. One final problem in this current model is that any net transport between two open boundaries needs to be prescribed in advance. This may not be a problem as such transports might be known to be small, for example the net northward transport in the North Atlantic. In domains where the net transport between two open boundaries does vary in time, the variation will almost certainly be affected by external factors which no open boundary condition could hope to calculate.

Current measurements are extremely variable and difficult to obtain accurately. Therefore it is not profitable to use them to set the vertical variation of velocity. This also has the disadvantage that the velocity field could be set in such a way that it is inconsistent with the density field. These two quantities are closely related through the equations of motion and in fact baroclinic waves propagate through the density field, so inconsistencies are undesirable. Fixing the baroclinic velocity field with some form of extrapolation could also lead to the same problem. With this in mind we calculate the baroclinic part of the velocity field on all open boundary points from the following linear form of the equations of motion (1) and (2),

$$\frac{\partial u}{\partial t} - fv = -\frac{1}{\rho_0 a \cos\phi}\frac{\partial p}{\partial \lambda} + F^u, \tag{9}$$

$$\frac{\partial v}{\partial t} + fu = -\frac{1}{\rho_0 a}\frac{\partial p}{\partial \phi} + F^v, \tag{10}$$

with F^u and F^v as described in Section 2. This avoids using unreliable current measurements and keeps the velocities consistent with the density field. The neglect of the nonlinear terms is justified by the fact that they are small in comparison with other terms in the equations. However there are certain regions in the ocean where the nonlinear terms are important, but it is sensible to choose open boundaries in positions away from such regions of intense activity. The neglect of these terms is also useful in that if they were retained, values of u, v and w which lie outside the boundary would need to be extrapolated from the open boundary values (which themselves are not exact) and any errors in the extrapolation would be compounded by the nonlinear nature of the terms. However without the linear diffusion term the solution is unstable. This term is retained by using a simple extrapolation for the unknown u and v.

Finally we need to fix the tracer quantities on the boundary, from which we can calculate the density. If the velocity at a certain level on an open boundary is directed out of the region then it is likely that the values of the tracers on the boundary are determined from inside the domain of interest. Thus we calculate the tracers from a simplification of (5), allowing a tracer quantity to be advected or diffused out of the interior. For simplicity tracers are only allowed to be advected out of the model region perpendicular to the boundary. The equation we use for this is

$$\frac{\partial T}{\partial t} + \frac{v}{a}\frac{\partial T}{\partial \phi} = F^T. \tag{11}$$

The scheme for tracers described above works to some extent but can be improved by a correction term to the velocity v. The correction is required because the upstream differencing used in the advective term inhibits the propagation of internal waves out through the boundary when the fluid is being advected inwards. This can then lead to a piling up of wave energy at the boundary. This effect will be illustrated in one of the examples below. The correcting phase speed c_T is calculated from the finite difference form of the equation

$$\frac{\partial T}{\partial t} = -\frac{c_T}{a}\frac{\partial T}{\partial \phi}, \tag{12}$$

at points adjacent to the boundary at the previous timestep for each level in the vertical. The revised equation used to calculate tracers when either v or c_T or both are in the direction out of the model region is

$$\frac{\partial T}{\partial t}+\frac{v+c_T}{a}\frac{\partial T}{\partial \phi}=F^T. \tag{13}$$

If v and F^T are neglected in (13) we are left with a radiation condition for T. However experiments have shown this is not sufficient to correctly model the behaviour of T at the boundary.

If the velocity on the boundary is into the domain of interest then there are two obvious choices. Either to let the tracer remain at its previous value which is suitable for a passive open boundary condition, or to set it to some prescribed value. For an active open boundary condition we need to continually force tracers at the boundary in certain places, so it is sensible to prescribe the value at the boundary. However this can lead to undesirable discontinuities in the vicinity of the boundary when the direction of the velocity at the boundary changes from outwards to inwards. Thus to eliminate this problem when the velocity is into the region of interest the tracer is smoothly forced towards its prescribed value by using the following equation

$$\frac{\partial T}{\partial t}=\alpha(T_b-T), \tag{14}$$

where T_b is the prescribed boundary value and α is some suitably chosen positive constant. If there are any problems close to the open boundary due to the sharpness of any of the fields it may be desirable to smooth this out by increasing the diffusion in that region. Improvements could be made to allow advection and wave propagation at oblique angles to the boundary, but for simplicity in this initial study the method described above is felt to be sufficient.

4. FINITE DIFFERENCE FORMULATION

The horizontal arrangement of grid points at a southern open boundary is shown in Figure 1. Points where the open boundary joins a solid boundary are treated no differently than interior ocean points that are adjacent to a solid boundary. For the stream function equation the standard model calculations are performed for all rows $J \geqq 2$. For an active open boundary condition the stream function is prescribed along row $J=1$. For a passive open boundary some form of extrapolation is required. A variation of the Orlanski (1976) boundary condition is used for the idealised test below. A phase speed c_ψ is calculated from the finite difference form of the equation

$$\frac{\partial \psi}{\partial t}=-\frac{c_\psi}{a}\frac{\partial \psi}{\partial \phi}, \tag{15}$$

at the previous timestep for points just inside the boundary. Leapfrog time stepping could easily have been implemented here, but as it requires holding an

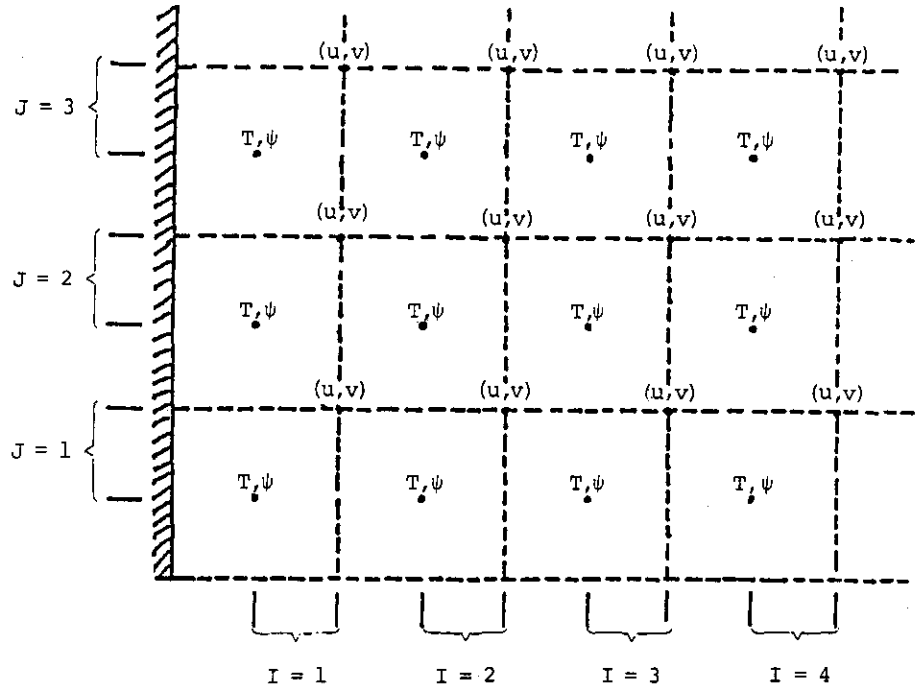

Figure 1 Horizontal arrangement of grid points at a southern open boundary.

extra time level in memory at points near the boundary, forward time stepping is used. It might be thought at this stage that this could lead to problems with mixing of modes at the boundary. However the reader is reminded that the use of the Robert time filter every time step effectively eliminates the computational mode. No such problems have been encountered in any of the tests so far performed. Further tests with an occasional Euler forward or Euler backward timestep to eliminate the computational mode, rather than the Robert time filter, also show no such problems. In fact any inaccuracies are more likely to come from the inadequacy of the radiation condition in modelling the stream function at the boundary. Further, analysis of various radiation conditions by Miller and Thorpe (1981) shows that this approach also leads to smaller local truncation errors at the boundary. If the phase speed c_ψ exceeds the maximum feasible numerical velocity $a\Delta\phi/\Delta t$ then it is set to that limit. If however the value of c_ψ suggests propagation into the model domain then c_ψ is set to zero. A new value of the stream function is then calculated from the same equation (15) for the points along the boundary. The formulation described above then reduces to the following

$$\psi_{i,1}^{n+1} = \psi_{i,1}^{n} + r(\psi_{i,2}^{n} - \psi_{i,1}^{n}), \tag{16}$$

where

$$r=0, \quad q\geqq 0,$$

$$r=q, \quad -1<q<0,$$

$$r=-1, \quad q\leqq -1,$$

and

$$q=\frac{\psi_{i,2}^{n}-\psi_{i,2}^{n-1}}{\psi_{i,3}^{n-1}-\psi_{i,2}^{n-1}}.$$

The usual model calculations for baroclinic motion and tracers take place for all rows $J\geqq 2$. On the boundary (9) and (10), describing baroclonic motion, are solved by the same procedure as is used for solving (1) and (2) with two exceptions. Firstly (9) and (10) do not contain the advective terms. Secondly the values of u and v at grid points just outside the model region are assumed to be equal to the value of those on the boundary for calculating the diffusion terms.

The equation to be solved for tracers also differs from that for a standard grid point by the advective term. However for this equation the advective term is important and is retained in a modified form with tracers only advected out of the basin perpendicular to the boundary. This term is written in a nonconservative form using upstream differencing which enables it to be retained without having to use values which would otherwise be unknown. The use of upstream differencing introduces an additional amount of damping [see O'Brien (1986) for details], which, in the examples presented below, is of a comparable magnitude to the diffusive term. The additional phase velocity c_T for each level k is calculated in a similar manner to that for the stream function described above. The correcting phase speed is

$$c_{Ti,k}^{n}=-\frac{a\Delta\phi}{\Delta t}\left[\frac{T_{i,2,k}^{n}-T_{i,2,k}^{n-1}}{T_{i,3,k}^{n-1}-T_{i,2,k}^{n-1}}\right], \tag{17}$$

for $-a\Delta\phi/\Delta t\leqq c_{Ti,k}^{n}\leqq 0$ with $c_{Ti,k}^{n}$ set to its bounds if its exceeds them. Again forward differences are used instead of leapfrogging for time differencing. The finite difference form of the equation for tracers is

$$\frac{T_{i,1,k}^{n+1}-T_{i,1,k}^{n}}{\Delta t}=-\left[\frac{c_{Ti,k}^{n}+v_{i,1,k}^{n}}{a}\right]\left[\frac{T_{i,2,k}^{n}-T_{i,1,k}^{n}}{\Delta\phi}\right]+F_{i,1,k}^{Tn}, \tag{18}$$

where $F_{i,1,k}^{Tn}$ is the usual diffusion term. The value of a tracer at the unknown point just outside the model domain is set equal to that on the boundary for the calculation of the diffusion term in passive open boundary condition. However this value can be set using hydrographic data (if it is available) when using an active open boundary condition.

Table 1 Temperature and salinities in the model basin

Level	*Depth metres*	*Southern half*			*Northern half*		
		Temperature °C	*Salinity* ppt	*Density* σ_θ	*Temperature* °C	*Salinity* ppt	*Density* σ_θ
1	25	10.3	35.053	26.98	4.6	34.500	27.36
2	150	6.7	35.125	27.60	−1.6	34.840	28.09
3	500	3.7	34.910	27.78	−1.1	34.890	28.11
4	1100	1.5	34.918	27.98	−1.1	34.898	28.12
5	1850	−0.45	34.912	28.10	−1.2	34.889	28.11
6	2700	−0.85	34.912	28.12	−1.2	34.889	28.11

5. A PASSIVE OPEN BOUNDARY CONDITION

In this section, and the following two, idealised tests of the proposed open boundary condition are described. In this test a passive open boundary condition is demonstrated where waves generated within the model domain are allowed to pass out through the boundary without distorting the interior. Three simple rectangular basins are set up with eastern and western boundaries closed. Two have open northern and southern boundaries while the other has an extended domain north and south which will be used for comparison. One of the models with open boundaries will not have the extra correction term to the velocity v in the tracer equation. This will be used to show the importance of that term. The extended basin model will be referred to as model A, the model with the full open boundary condition will be referred to as B and the model with the missing correction term (that is with tracers calculated using (11)) as C. The basins are centred on 62.25 degrees North. The grid size is 1 degree in the zonal direction and 0.5 degree in the meridional direction, which is approximately 55 km in both directions at this latitude. In the vertical the grid size varies from 50 metres at the surface to 900 metres at the bottom and the timestep is 2400 seconds. The horizontal mixing coefficients A_m and A_h are chosen to be $10^8\,\mathrm{cm^2\,s^{-1}}$ and $5\times10^6\,\mathrm{cm^2\,s^{-1}}$ respectively and the vertical mixing coefficients K_m and K_h are both chosen to be $1\,\mathrm{cm^2\,s^{-1}}$. The rather large value of A_m is chosen for computational stability [see Bryan *et al.* (1975) and Killworth *et al.* (1984) for details] to allow formation of lateral boundary currents and inhibit the computational mode caused by central differencing. There is no forcing at the surface during this test. At the initial instant the fluid in the basin is at rest but the northern and southern halves are filled with fluid of different densities (see Table 1). The values of temperature and salinity used were based on data from GEOSECS (Bainbridge, 1980) stations 17 and 19 in the Norwegian sea. Two baroclinic Kelvin waves are immediately formed, one travelling north along the eastern boundary and one travelling south along the western boundary. The internal radius of deformation is approximately 20 km, whereas the grid spacing is much wider. Thus as Hsieh and Gill (1984) point out the effect of the above, combined with large values of A_m and A_h, leads to a much wider, slower baroclinic Kelvin wave than would otherwise be expected. These waves should be able to propagate out of the region without being reflected or modified.

To illustrate the results produced, the temperature field at level 2 (150 metres) will be shown at various times for the three models. The choice of level 2 is totally arbitrary as the results are similar for any level. Figure 2 shows the temperature field after 22.2 days, the front of the Kelvin wave has just reached the boundary of the open boundary models. There is no noticeable difference in the temperature field between models A and B. However in model C there is a small amount of distortion in the south western corner. After 55.5 days (Figure 3) there is still no noticeable difference between models A and B, the Kelvin waves appear to have successfully passed through the open boundaries of model B. However there is now a considerable amount of distortion along the south western coast and a small amount in the north eastern corner of model C. The boundary condition in model C has certainly acted better than a solid wall by allowing the wave to pass through and in fact appears to have done quite well in the North. This is because the velocity field at the level shown is advecting fluid in the same direction as the propagating Kelvin wave in the North and thus the value on the boundary is being freely modified. However in the South, fluid is advected in from outside the model domain thus fixing the temperature field and thus inhibiting the propagation of the Kelvin wave. Figure 4 shows the temperature field after a much greater time, 111 days. Once more model B has emulated model A well except for the re-emergence of the Kelvin wave in the south eastern corner of the extended model after travelling right around the basin. This is obviously not reproduced by the open boundary model as it is produced by an effect originating outside the model domain. Once again there is some distortion in the south western corner and to a lesser extent the north eastern corner of model C, however it does not affect the interior solution very much due to the smoothing effect of diffusion. The barotropic stream function is also shown after 111 days (Figure 5). Here the agreement between the models is not quite so good but nevertheless the result is reasonable. This disagreement is probably due to the fact that the radiation condition used here does not model the physics of the stream function that well, and in fact can be thought of as just a glorified extrapolation scheme. Finally a history plot of salinity for a point at level 4 on the coast one grid point in from the position of the northern open boundary is shown in Figure 6. The position of this point is marked by a cross on Figures 5(a) and (b). It can be seen that model B's salinity (dashed line) emulates that of model A (solid line) extremely well during the first 4000 timesteps.

6. AN ACTIVE OPEN BOUNDARY CONDITION

For the second test an active condition where the open boundary plays an important role in forcing the region of interest is demonstrated. A mid-latitude basin centred on 35 degrees North is set up. The basin is discretised in the following way; the horizontal grid spacing is 2 degrees in both the meridional and zonal directions, with 20 grid points in each direction. There are six levels in the vertical varying from 50 metres at the surface to 1200 metres at depth. The timestep for the internal and external mode velocities is 7200 seconds while the slowly varying tracer field has a longer timestep of 172 800 seconds (two days).

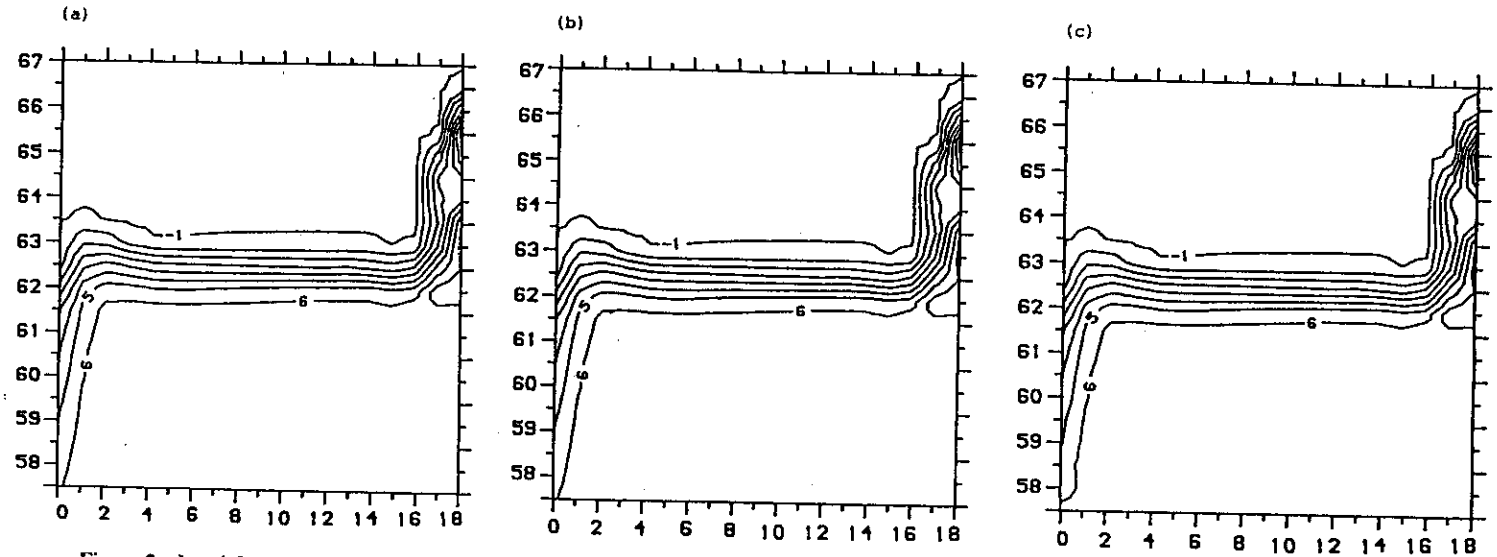

Figure 2 Level 2 temperature (in degrees C) for the three models A, B and C after 22.2 days. (a) model A, (b) model B and (c) model C.

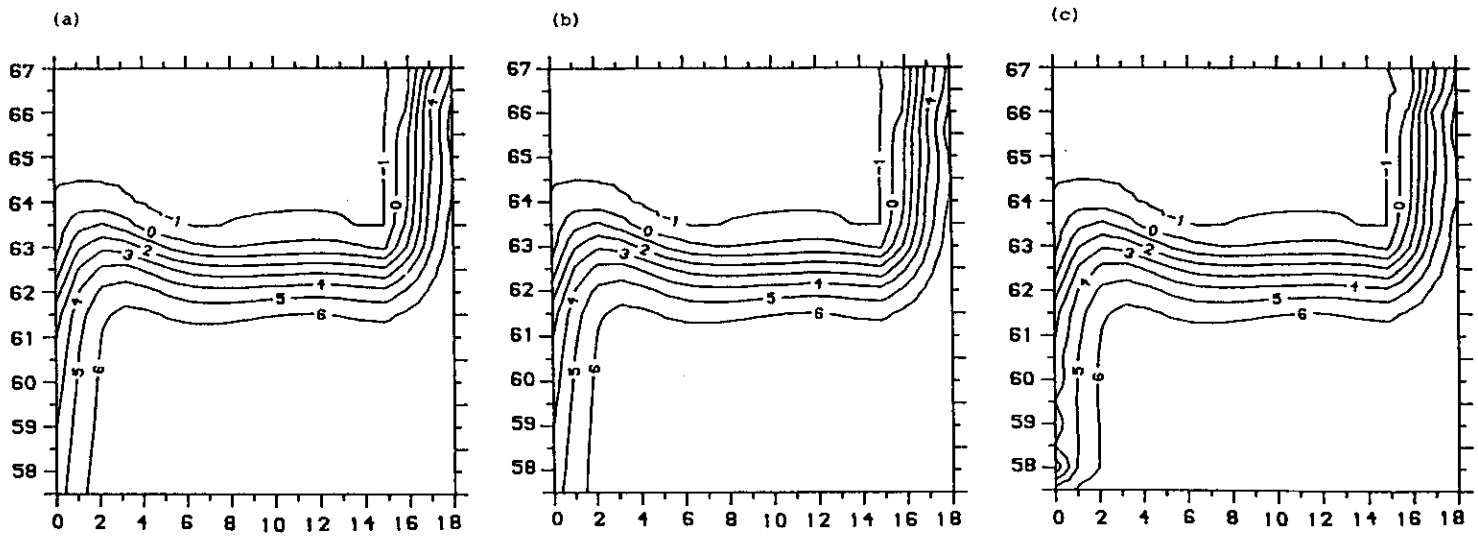

Figure 3 Level 2 temperature (in degrees C) after 55.5 days for the three basins (a), (b), (c) of Figure 2.

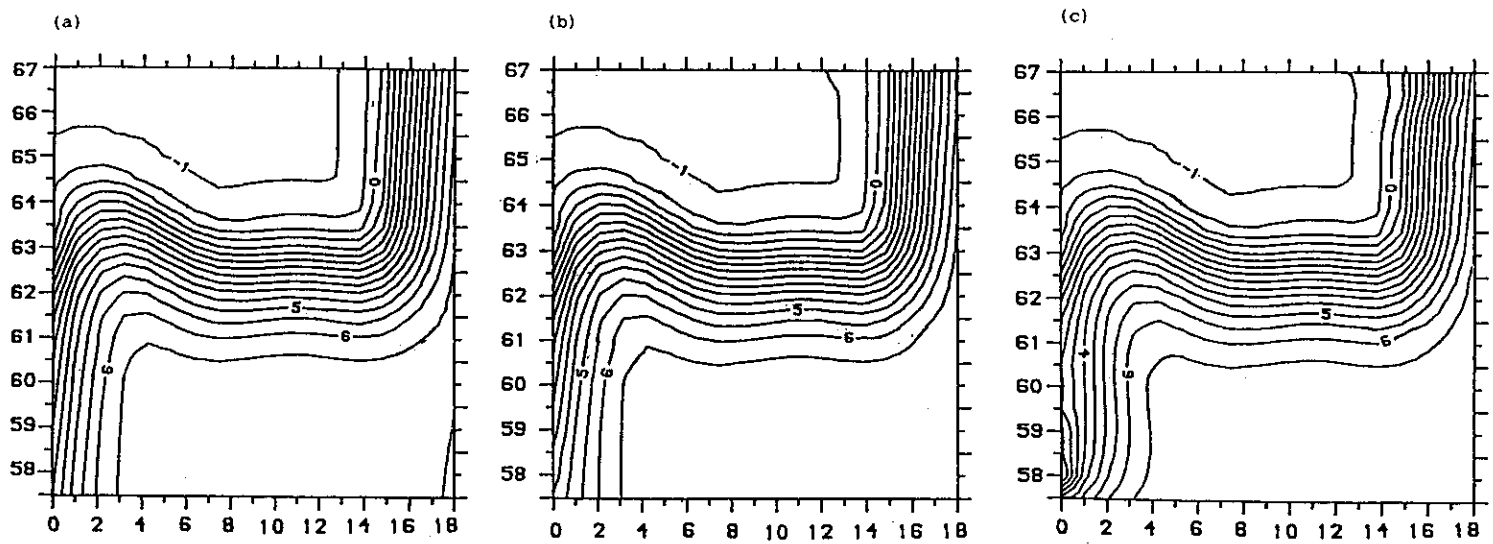

Figure 4 Level 2 temperature (in degrees C) after 111 days for the three basins (a), (b), (c) of Figure 2.

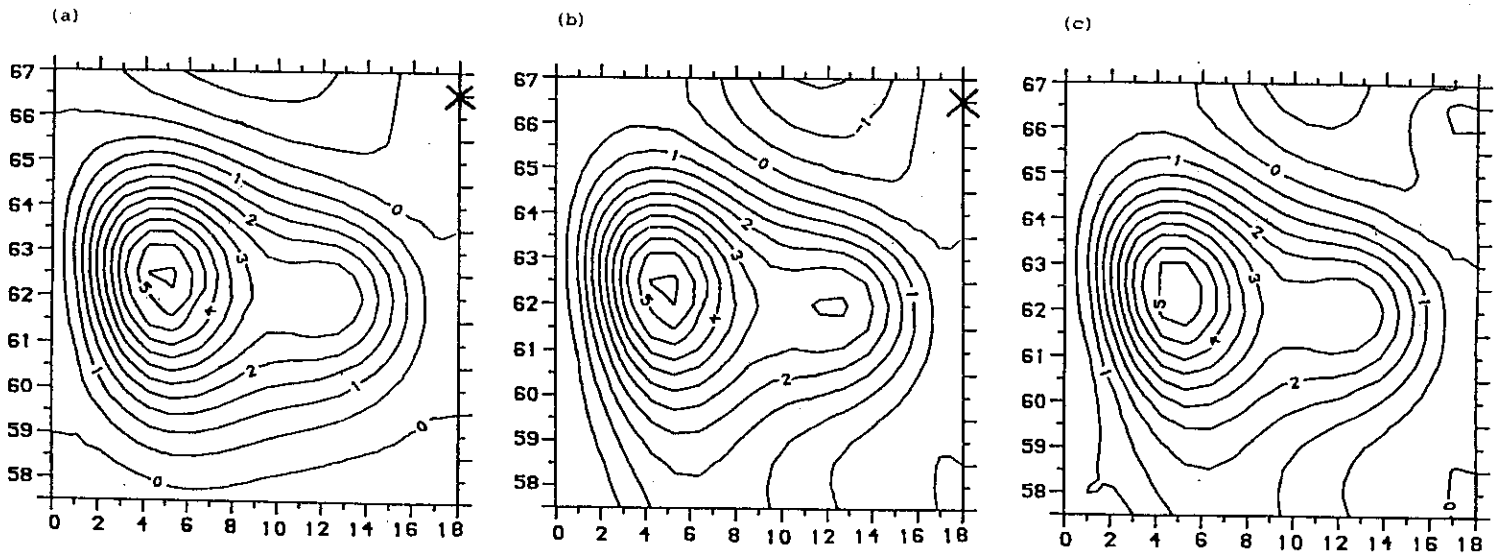

Figure 5 Barotropic stream function (in Sverdrups) after 111 days for the three basins (a), (b), (c) of Figure 2.

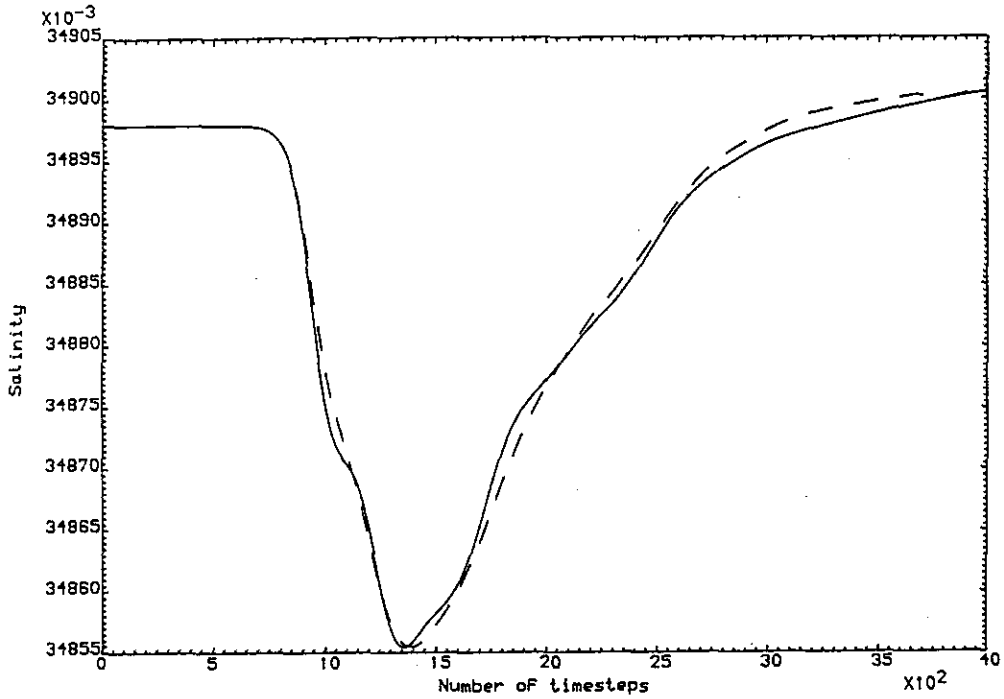

Figure 6 History plot of salinity (in ppt) for a point on the coast just inside the northern open boundary at level 4. Open boundary model dashed line, extended basin model solid line.

The horizontal mixing coefficients A_m and A_h are $10^9\,\mathrm{cm^2\,s^{-1}}$ and $2\times10^7\,\mathrm{cm^2\,s^{-1}}$, once more the vertical mixing coefficients K_m and K_h are both chosen to be $1\,\mathrm{cm^2\,s^{-1}}$. Again the large values of A_m and A_h are for computational stability. The basin is filled with fluid at a temperature of 6 °C and salinity 34.9 ppt. A wind stress of the form

$$\tau^{\lambda} = -0.1\cos\left(\pi\frac{\phi-\phi_1}{\phi_2}\right)\mathrm{Nm^{-2}}, \tag{19}$$

$$\tau^{\phi} = 0\,\mathrm{Nm^{-2}}, \tag{20}$$

and a surface temperature and salinity of the form

$$\theta = 27-25\left(\frac{\phi-\phi_3}{\phi_4}\right)^{\circ}\mathrm{C}, \tag{21}$$

$$S = 35.0 + 0.7 \sin\left(2\pi \frac{\phi - \phi_3}{\phi_4}\right) \text{ppt}, \tag{22}$$

where $\phi_1 = 0.297, \phi_2 = 0.559, \phi_3 = 0.279$ and $\phi_4 = 0.593$ radians, are applied at the surface and the basin is spun up. This results in a classic Stommel-type gyre with a western boundary current. Hereafter this will be referred to as model D. After approximately 1700 years when the ocean is in a steady state the run is stopped. The stream function is noted at all points across the basin at the halfway point north south. The temperature and salinity are also noted as if a hydrographic section had been taken across the basin.

Three further basins of half the size of model D corresponding to the northern half are then filled with fluid of temperature 6 °C and salinity 34.9 ppt. The first of these basins has an active open boundary along its southern side, this will be referred to as model E. The steady state values of temperature and salinity from model D are fed into the model through the open boundary condition as T_b in (14). Additionally hydrographic data is used for the unknown term in the tracer diffusion calculation. The stream function is specified using data from model D. This run is to illustrate how the open boundary condition performs with accurate, albeit steady state, boundary data. A second similar run, model F, is undertaken. However this time the Sverdrup balance is used to specify the stream function. In addition a western boundary current is imposed to give no net northward transport across the open boundary and hence ensure conservation of mass. This model is to test the open boundary in a more realistic situation, that is giving the ocean model nothing more than hydrographic and wind data. Finally for comparison purposes a model is set up with all its variables prescribed along the southern boundary using steady state values from model D. This model hereafter referred to as model G has thus been given much more information than models E and F.

These three basins are then spun up from the same initial state as model D using the same forcing for the same length of time. The resulting stream function fields are shown in Figure 7. Models E and G which had exact stream function data at the open boundaries have emulated the stream function of model D extremely well. This is hardly surprising as the stream function field responds very quickly to the dominating wind forcing and is only affected a minimal amount by the baroclinic and tracer fields which take much longer to evolve. In fact the problem for the stream function could almost be thought of as a steady elliptic problem with exact data along the open boundary for most of the run and hence good results are almost inevitable. Model F in which the Sverdrup balance was used is not quite as good but nevertheless has done well, the average error in stream function over the half basin is less than 5%. The strength of the return southwards flow and thus the strength of boundary current is slightly underestimated. This causes a small amount of distortion to the east of the boundary current near the open boundary. Figure 8 shows the temperature field at level 3 for all four models. The open boundary condition models E and F have performed well in reproducing the isotherms of model D, the mean error is approximately 1%

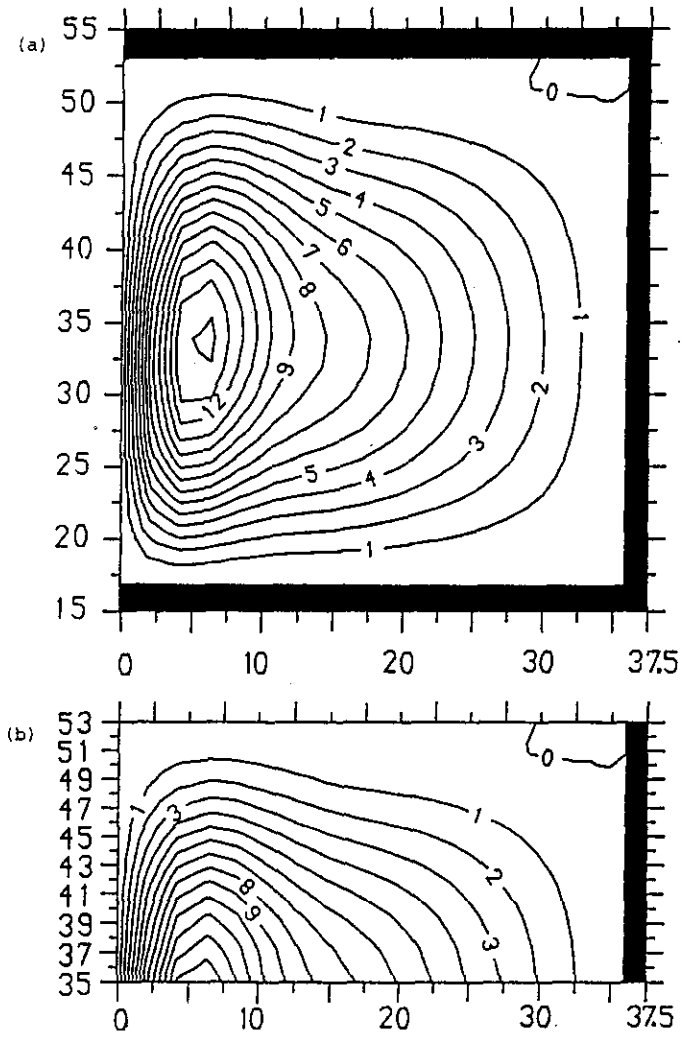

Figure 7 Barotropic stream function (in Sverdrups) for the four models D, E, F and G. (a) model D, (b) model E, (c) model F and (d) model G.

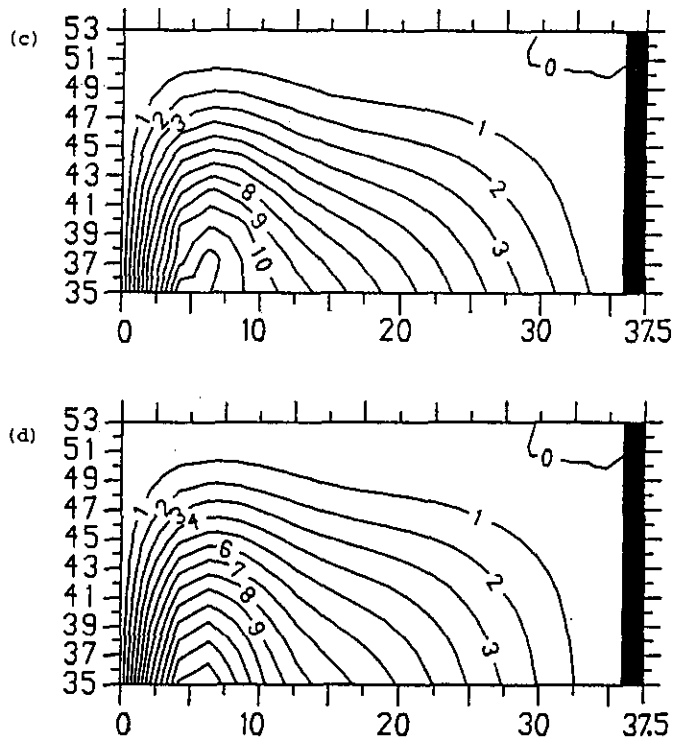

Figure 7 Barotropic stream function (in Sverdrups) for the four models D, E, F and G. (a) model D, (b) model E, (c) model F and (d) model G.

in both cases. Model G with prescribed values along the open boundary has done even better. The salinity fields for level 2 are shown in Figure 9. Once more the open boundary condition models E and F have accurately predicted the structure of the salinity field, while model G has performed the best. Thus it seems that steady prescribed data along an open boundary will give the correct steady solution after spinning up. However it must be remembered that we will probably never have such good velocity data in a real situation. We are more likely to find ourselves in a situation such as model F with temperature, salinity sections and wind data.

7. A TROPICAL OCEAN MODEL

For this test three tropical ocean basins, centred on the equator, were set up. This test is of interest as it includes the rather complex tropical dynamics and the outflow of forced waves. Further it tests the open boundary condition in another situation where it may be realistically used, namely a zonal tropical ocean band. The largest, model H, was closed and extended from 18 °S to 18 °N. The second, model I, has zonal passive open boundaries and extended from 7 °S to 7 °N. The

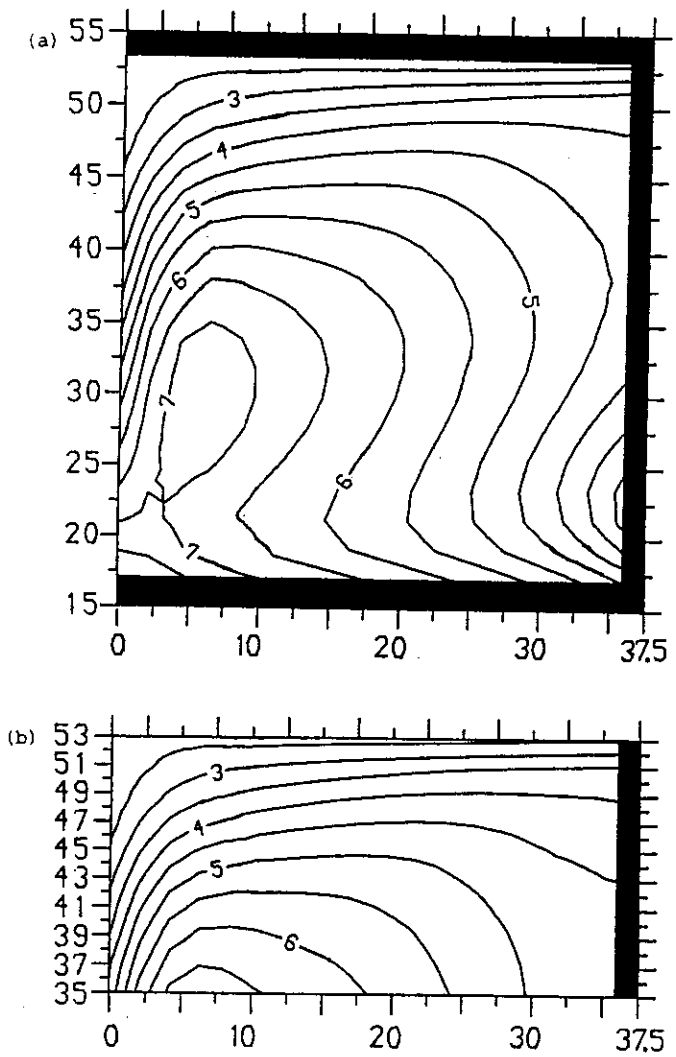

Figure 8 Temperature (in degrees C) at level 3 for the four models, (a), (b), (c) and (d) of Figure 7.

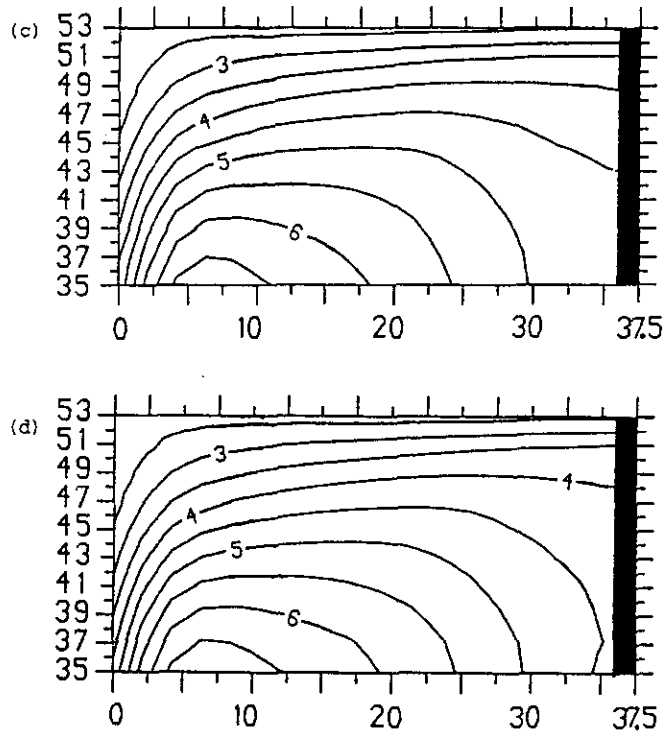

Figure 8 Temperature (in degrees C) at level 3 for the four models, (a), (b), (c) and (d) of Figure 7.

third, model J, also had zonal passive open boundaries but only extended between 4°S and 4°N. The east–west extent of all three basins is 28°. A horizontal grid spacing of 1 degree in both meridional and zonal directions was chosen. There were six levels in the vertical with grid spacing varying between 50 metres at the surface and 1200 metres at depth. A timestep of 90 minutes was used for all variables. The mixing coefficients A_m, A_h, K_m and K_h of Section 5 were used. The basins were initialised with a spatially homogeneous temperature profile (see Table 2) and zero velocity. The effects of salinity are not included. A constant easterly wind stress of $0.05\,\mathrm{Nm}^{-2}$ was specified at the ocean surface. The Sverdrup balance provides no useful information, thus the radiation condition described in Section 4 will be used to calculate the stream function at the boundary. It should be pointed out that the barotropic response is not important in tropical regions and is often removed, thus eliminating the most troublesome part of the open boundary condition. However it is retained in this present study for completeness. Only the portion of the ocean north of the equator will be illustrated because of the symmetry involved.

A brief (and basic) description of the physics involved in model H with the

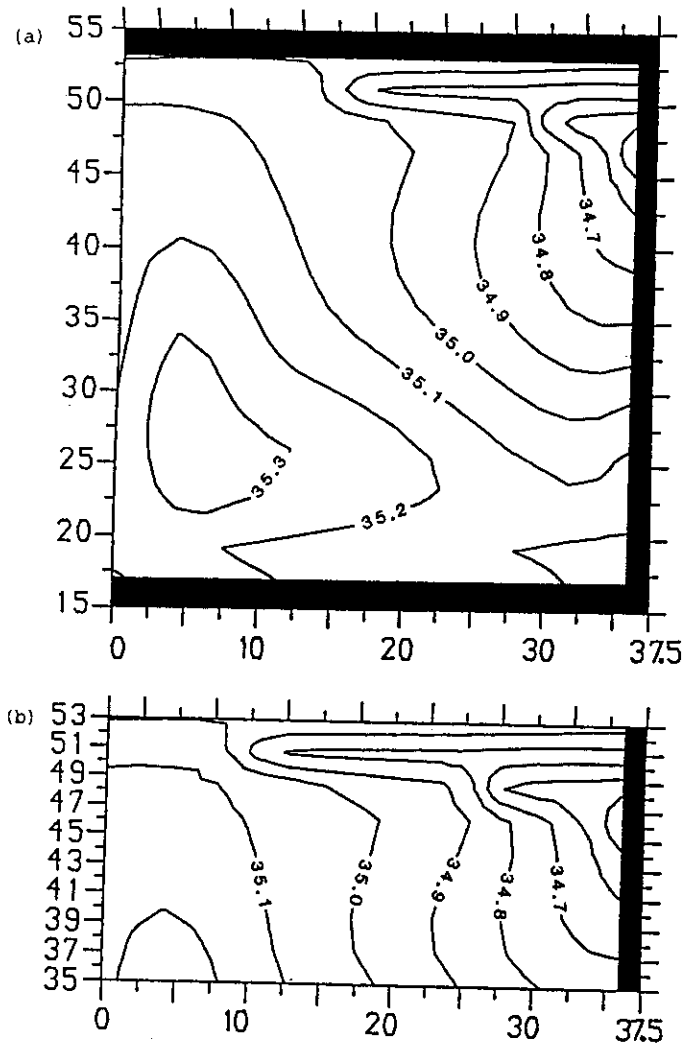

Figure 9 Salinity (in ppt) at level 2 for the four models, (a), (b), (c) and (d) of Figure 7.

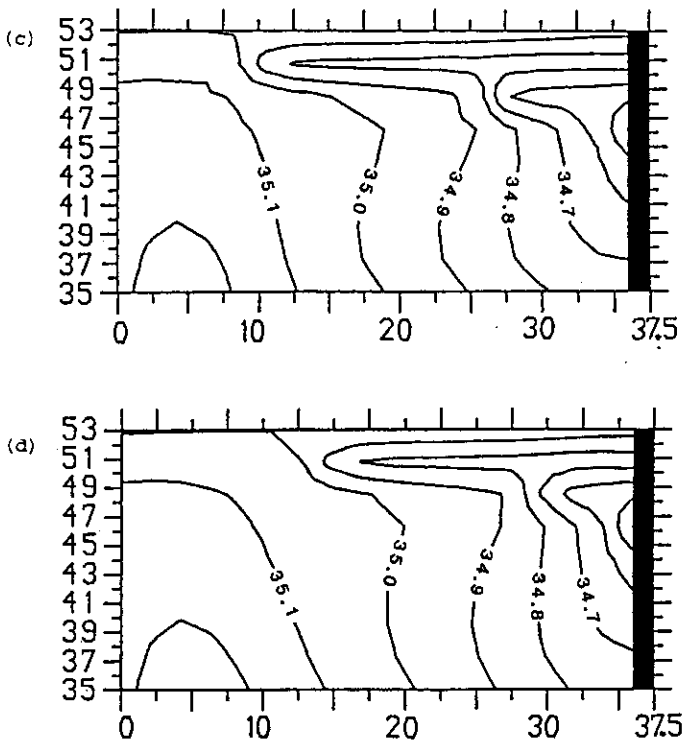

Figure 9 Salinity (in ppt) at level 2 for the four models, (a), (b), (c) and (d) of Figure 7.

Table 2 Initial temperature profile in the model basins

Level	*Depth metres*	*Temperature °C*
1	25	25.0
2	150	10.0
3	500	8.0
4	1150	6.3
5	2050	4.6
6	3150	3.0

closed basin will now be given. The imposed wind stress causes a poleward transport in the surface Ekman layer. This leads to divergence at the equator causing equatorial upwelling, while downwelling is caused at the northern boundary. A coastal Kelvin wave associated with the downwelling is generated at the northern boundary. A further coastal Kelvin wave is excited travelling poleward along the eastern boundary from the equator, while a Rossby wave propagates westwards along the equator from the eastern boundary. An equatorial Kelvin wave travels along the equator from west to east. On reaching the eastern

boundary, reflection occurs producing a westward propagating Rossby wave, while a coastal Kelvin wave propagates northwards along the eastern boundary.

To illustrate the results produced, the temperature field at level 2 (150 metres) will be shown at various times for all three models. At one week (Figure 10) upwelling along the equator due to the wind stress is noticeable in all three models. The coastal Kelvin wave that propagates northwards up the eastern boundary is also visible. Additionally in model H downwelling is apparent at the northern boundary along with the associated Kelvin wave which is beginning to propagate toward the equator along the western boundary. Model I is reproducing model H satisfactorily, however model J is not fairing so well. After five weeks (Figure 11) the Kelvin wave propagating northwards along the eastern boundary has passed through the open boundaries of models I and J. It passed through the boundary of model I without causing any distortion whatsoever. However problems seem to be occurring with model J, not only in the region of the Kelvin wave but throughout the entire domain. The coastal Kelvin wave generated on the northern boundary has started to move southwards along the western boundary. There is now evidence of an equatorial Kelvin wave, which can be distinguished by the 11.5 °C contour, propagating along the equator. Finally after 9 weeks (Figure 12) the coastal Kelvin wave from the northern boundary of model H is just about to enter the domain of model I. Further integration would be pointless as this wave which does not occur in models I and J will interact with other phenomena and hence change the solution. However at this stage model I is still performing well, the isotherms of model H are faithfully reproduced. The equatorial Kelvin wave has just reached the eastern boundary. The interaction with the boundary has produced a westward travelling Rossby wave and a poleward travelling Kelvin wave. Model J has now become totally contaminated, with the isotherms bearing only the slightest resemblance to those of models H and I.

The barotropic stream function at 784 timesteps (7 weeks) is illustrated in Figure 13. Model H has two distinct gyres, one of cyclonic circulation in the west and one of anti-cyclonic circulation in the east. These gyres have been accurately reproduced (both quantitatively and qualitatively) by model I although there is a small discrepancy near the boundary. Once more model J has not performed so well. Both gyres are present, but they are more intense.

Overall model I has performed well, illustrating that the condition works successfully for the forced wave problem. The failure of model J can probably be put down to the following reason. The open boundary is in a position where the flow and wave propagation are tangential to the boundary. It must be remembered that the condition as it stands requires flow and propagation perpendicular to the boundary. Thus it is sensible to think about the positioning of open boundaries based on some knowledge of the dynamics expected. Failure to do so could lead to results such as model J rather than those of model I.

8. CONCLUSION

An open boundary condition has been constructed for use with three dimensional

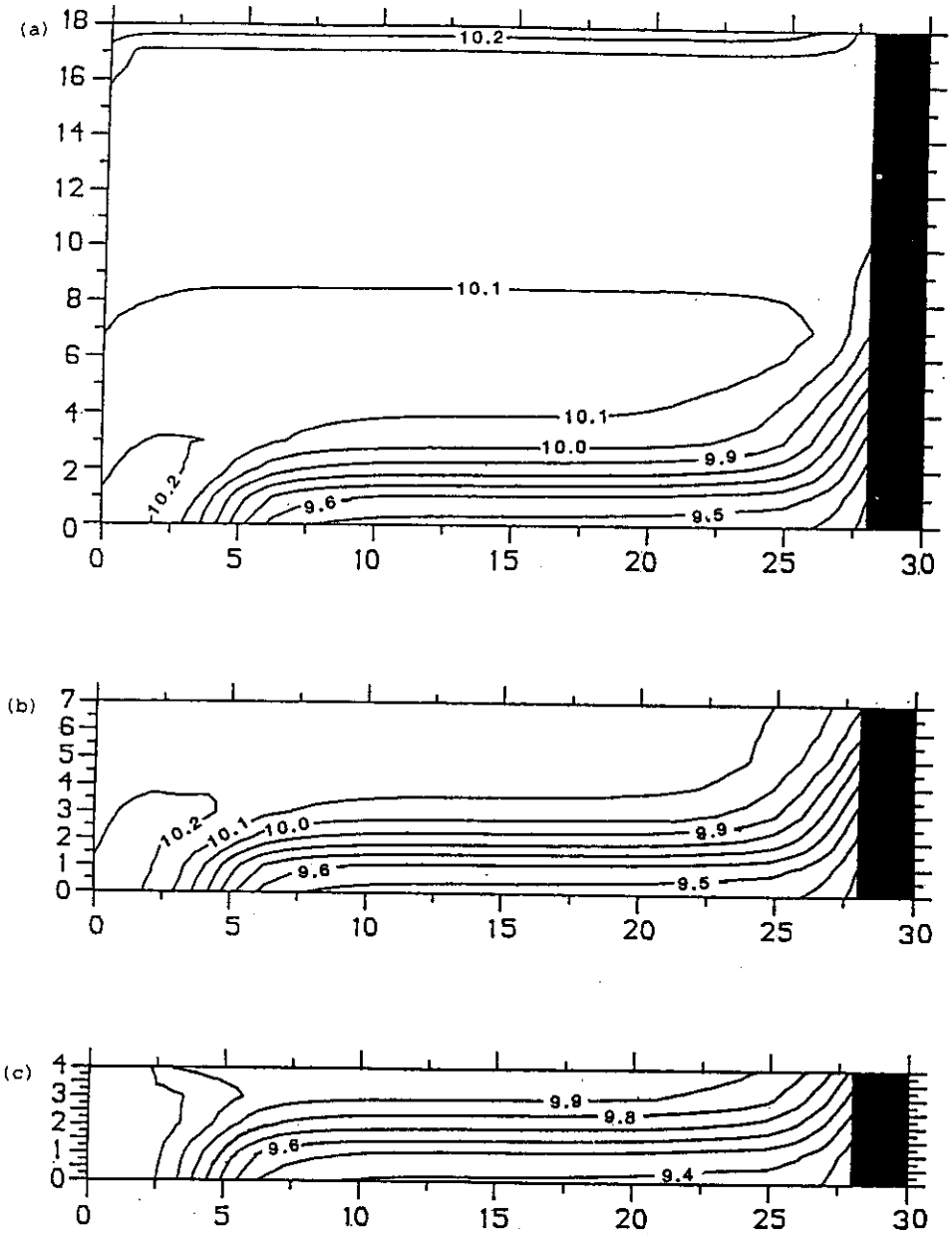

Figure 10 Temperature (in degrees C) at level 2 after 1 week for the three models H. I and J. (a) model H, (b) model I and (c) model J.

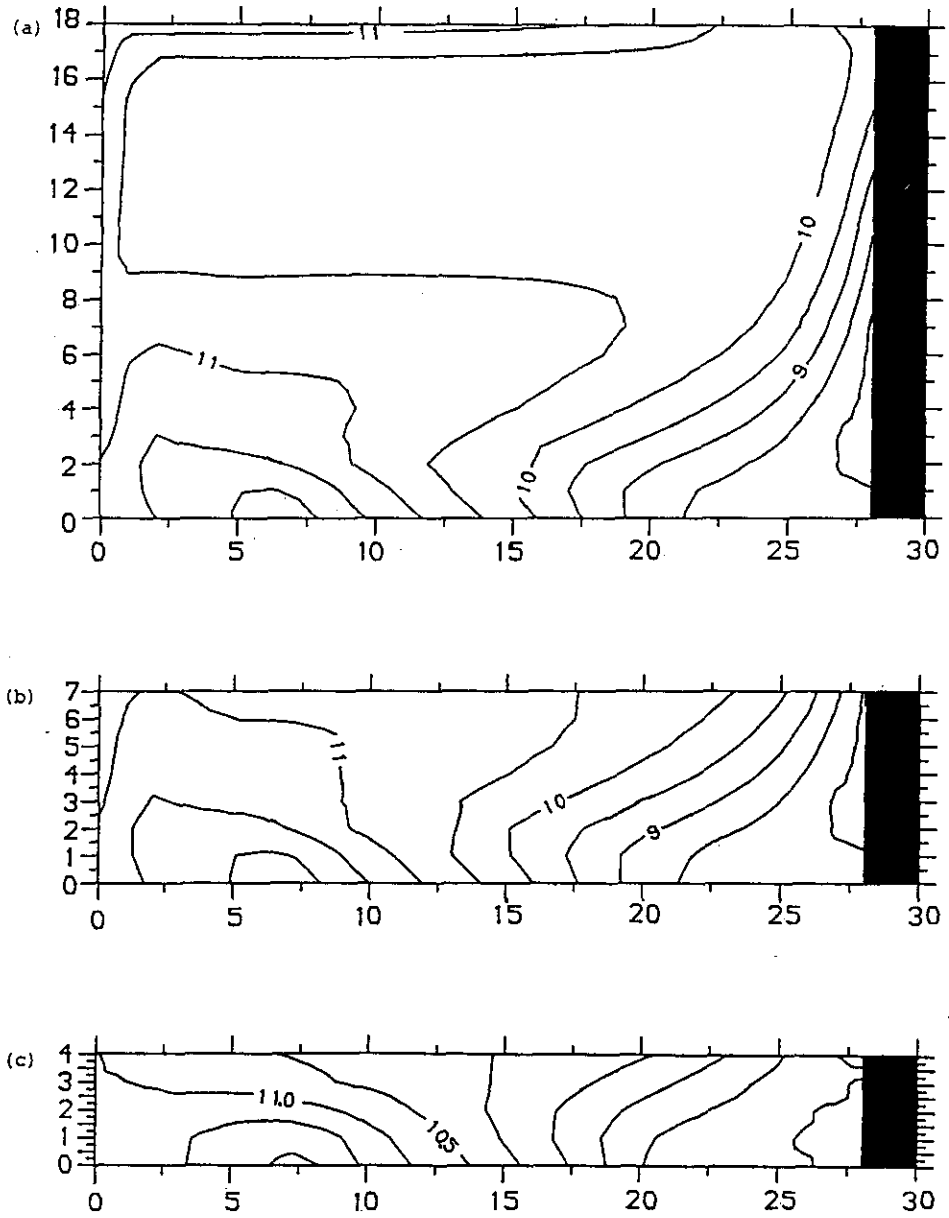

Figure 11 Temperature (in degrees C) at level 2 after 5 weeks for the three models, (a), (b) and (c) of Figure 10.

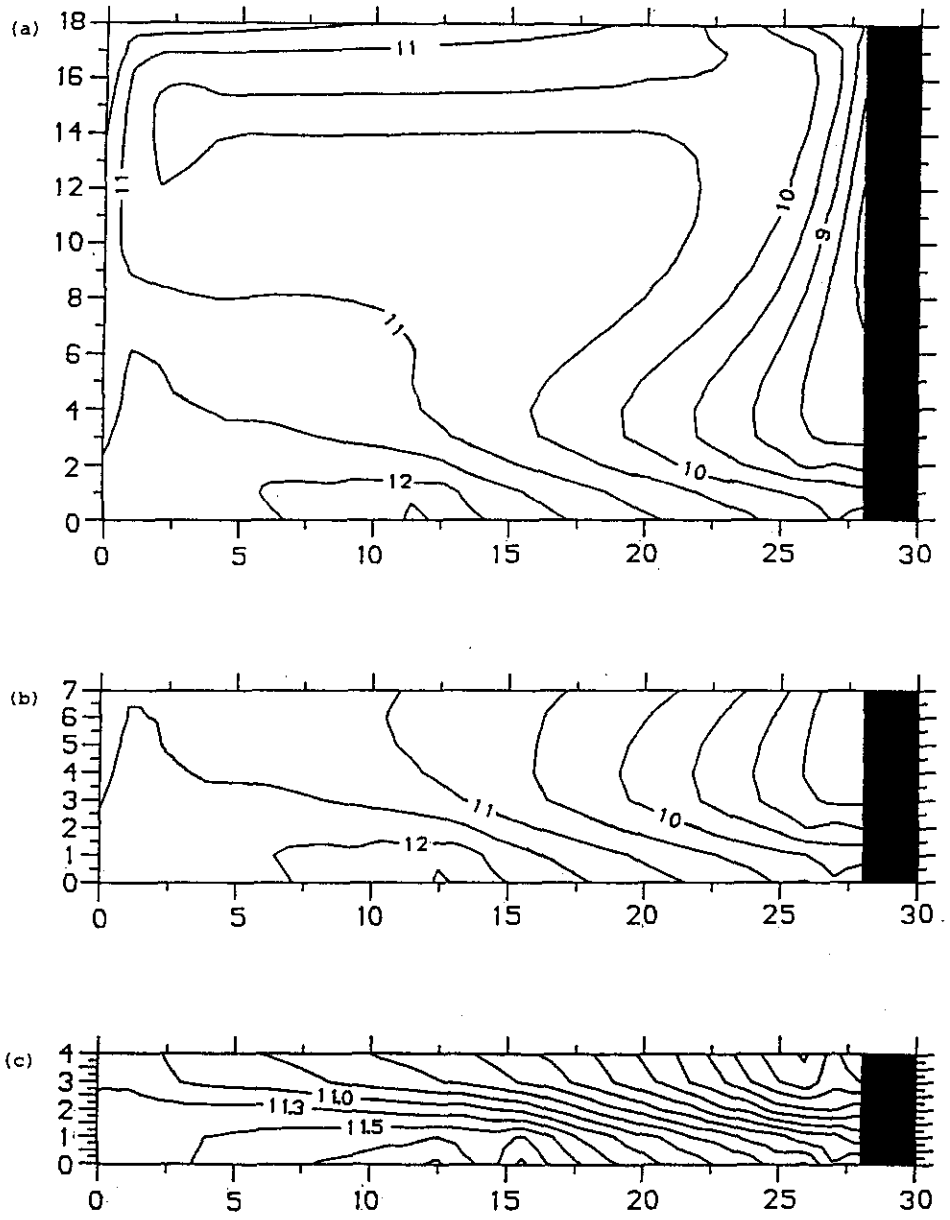

Figure 12 Temperature (in degrees C) at level 2 after 9 weeks for the three models, (a), (b) and (c) of Figure 10.

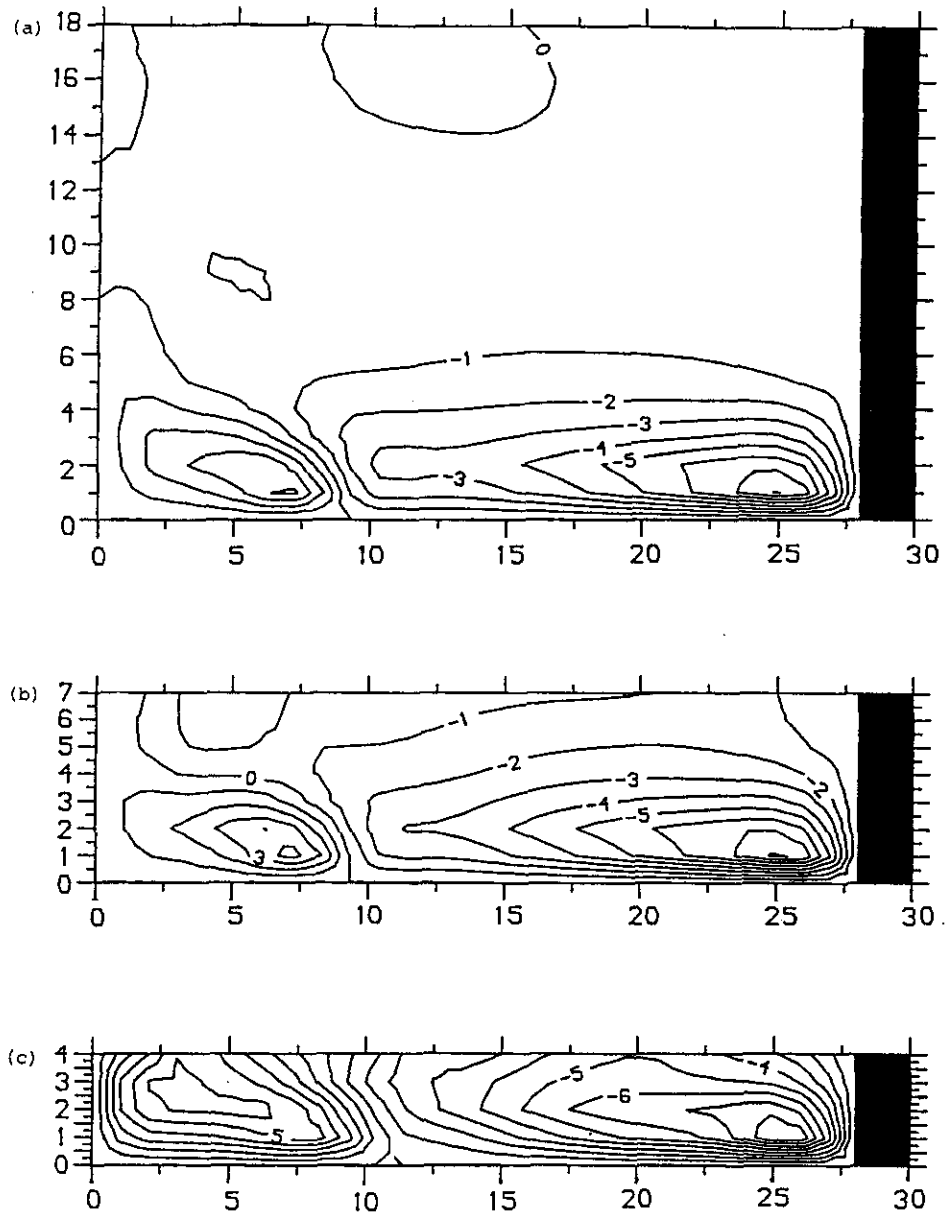

Figure 13 Barotropic stream function (in Sverdrups) after 7 weeks for the three models, (a), (b), (c) of Figure 10.

primitive equation models. The boundary condition can be used in two forms, as an active open boundary condition which forces the interior domain or as a passive one in which phenomena generated within the model domain can leave without distorting the interior solution. Three tests have been performed to test the boundary condition in both forms; none of the tests used enhanced diffusion in the area of the boundary. The first test works extremely well for tracer and baroclinic fields. The boundary condition allows Kelvin waves to propagate out of the model domain without affecting the interior solution in any way. The results are less good for the stream function. This is not surprising since the elliptic equation to be solved for the stream function cannot easily be simplified to obtain a prediction equation for ψ on the boundary.

The second example is a far more severe test of the open boundary condition. The stream function field is predicted very accurately. The temperature and salinity fields are also well reproduced by the model with an open boundary condition. Prescribing variables to steady values produced the best results, but in reality are we likely to get accurate current measurements across such large sections? The open boundary condition model managed to produce good results just using ideal "climatological" temperature and salinity data which is already available for much of the world's oceans and so is a much more realistic prospect.

The third example illustrates the use of the open boundary condition in the tropics. This example also provided a test of the open boundary condition with forced waves. Once more the open boundary condition performed well. This example also demonstrated that some thought should be taken over the positioning of open boundaries (at least in their present form) based on knowledge of the expected dynamics. Namely they should be away from regions where the flow or propagation is locally tangential to the boundary or regions of intense activity. The use of heat fluxes in closed domain models of the tropics leads to a continual warming of the ocean, rendering longterm integrations useless. However the use of the open boundary condition enables a realistic poleward transport of heat out of the model domain. This has been verified in a 150 year long integration, which showed no significant warming of the ocean.

Only steady wind forcing has been tested so far, although it is felt that using the Sverdup balance and allowing for boundary currents would be a good enough boundary condition for the quickly responding barotropic stream function in cases where there is wind forcing varying with time. This has been found to be the case by Dr P. Killworth (Personal Communication) with the U.K. Fine Resolution Antarctic Model. Allowing temperature and salinity at the boundary to vary with time should also be fairly easy to implement for active open boundary conditions.

Although the condition was developed with a model of the Norwegian and Greenland Seas in mind, the results of the tests suggest the condition will be more widely applicable. The open boundary condition is currently being used in a number of models including the authors Norwegian–Greenland Sea model and the U.K. Fine Resolution Antarctic Model. These studies produce results which compare satisfactorily with observations, supporting the usefulness of the condition.

At present the open boundary condition only allows for advection of tracers in

a direction perpendicular to the boundary. It should be possible in the future to allow (with a modest amount of extrapolation) for advection of tracers in any direction across the boundary. More importantly there are schemes available which allow calculation of phase speeds at any angle to the boundary (Røed and Cooper (1986). These could be adapted for the tracer equation to allow internal waves to propagate out of the model domain at any angle without reflection. The addition of nonlinear terms in the momentum equations (9) and (10) is also possible, using the same technique as that in the tracer equations. This would hopefully improve the condition in situations where nonlinearity is important. Further tests on the condition, in more exacting (and realistic) situations, are planned in the future to aid development of the model.

Acknowledgements

The author wishes to thank Dr John Johnson for helpful discussion and guidance during this work.

References

Asselin, R., "Frequency filter for time integrations," *Mth. Wea. Rev.* **100,** 487 (1972).

Bainbridge, A. J., *GEOSECS Atlantic Expedition, Vol. 2, Sections and Profiles*, National Science Foundation, Washington, D.C. (1980).

Bennett, A. F. and Kloeden, P. E., "Boundary conditions for limited area forecasts," *J. Atmos. Sci.* **35,** 990 (1978).

Bryan, K., "A numerical method for the study of the circulation of the world ocean," *J. Comp. Phy.* **4,** 347 (1969).

Bryan, K., Manabe, S. and Pacanowski, R. C., "A global-atmosphere climate model. Part II. The oceanic circulation," *J. Phys. Oceanogr.* **5,** 30 (1975).

Camerlengo, A. L. and O'Brien, J. J., "Open boundary conditions in rotating fluids," *J. Comp. Phy.* **35,** 12 (1980).

Cox, M. D., "A primitive equation, 3-dimensional model of the ocean," *GFDL Ocean Group Tech Rep. No. 1* (1984).

Holland, W. R., "Quasigeostrophic modelling of eddy-resolved ocean circulation," In: *Proceedings of the NATO Advanced Study Institute on Advanced Physical Oceanographic Numerical Modelling* (J. J. O'Brien, ed.), D. Reidel Publishing Co., Dordrecht, (1986), p. 203.

Hsieh, W. W. and Gill, A. E., "The Rossby adjustment problem in a rotating, stratified channel, with and without topography," *J. Phys. Oceanogr.* **14,** 424 (1984).

Killworth, P. D., Smith, J. M. and Gill, A. E., "Speeding up ocean circulation models," *Ocean Modelling*, Unpublished manuscript (1984).

Miller, M. J. and Thorpe, A. J., "Radiation conditions for the lateral boundaries of limited-area numerical models," *Quart. J. R. Met. Soc.* **107,** 615 (1981).

O'Brien, J. J., "The hyperbolic problem," In: *Proceedings of the NATO Advanced Study Institute on Advanced Physical Oceanographic Numerical Modelling* (J. J. O'Brien, ed.), D. Reidel Publishing Co., Dordrecht (1986), p. 165.

Orlanski, I., "A simple boundary condition for unbounded hyperbolic flows," *J. Comp. Phy.* **21,** 251 (1976).

Røed, L. P. and Cooper, C. K., "Open boundary conditions in numerical ocean models," In: *Proceedings of the NATO Advanced Study Institute on Advanced Physical Oceanographic Numerical Modelling* (J. J. O'Brien, ed.), D. Reidel Publishing Co., Dordrecht (1986), p. 411.

Røed, L. P. and Smedstad, O. M., "Open boundary conditions for forced waves in a rotating fluid," *SIAM J. Sci. Stat. Comput.* **5,** 414 (1984).

Semtner, A. J., "An oceanic general circulation model with bottom topography," *UCLA Dept. of Meteorology Tech. Rep. No. 9* (1974).

Semtner, A. J., "Finite-difference formulation of a world ocean model," In: *Proceedings of the NATO Advanced Study Institute on Advanced Physical Oceanographic Numerical Modelling* (J. J. O'Brien, ed.), D. Reidel Publishing Co., Dordrecht (1986), p. 187.

Verron, J., "Use of open boundary conditions for the numerical simulation of an ocean box model," *Oceanol. Acta* **9**, 415 (1986).